Applied Catalysis B: Environmental 199 (2016) 331–341

Contents lists available at ScienceDirect

Applied Catalysis B: Environmental

journal homepage: www.elsevier.com/locate/apcatb

Effect of the anode materials on the efficiency of the electro-Fenton process for the mineralization of the antibiotic sulfamethazine

Flamur Sopaj[a,b], Nihal Oturan[a], Jean Pinson[c], Fetah Podvorica[b], Mehmet A. Oturan[a,*]

[a] Université Paris-Est, Laboratoire Géomatériaux et Environnement (EA 4508), UPEM, 5 Bd Descartes, Cedex 2, 77454 Marne-la-Vallée, France
[b] Chemistry Department of Natural Sciences Faculty, Europe University of Prishtina, rr. "Nëna Tereze" nr. 5, 10 000 Prishtina, Republic of Kosovo
[c] Univ Paris Diderot, Sorbonne Paris Citeí, ITODYS, UMR 7086 CNRS, 15 rue J-A de Baïf, 75205 Paris, Cedex 13, France

ARTICLE INFO

Article history:
Received 19 April 2016
Received in revised form 6 June 2016
Accepted 10 June 2016
Available online 14 June 2016

Keywords:
Sulfamethazine
Electro-Fenton
Anode material
Mineralization
Hydroxyl radicals

ABSTRACT

The role of anode materials on the electrochemical oxidation and mineralization of the antibiotic sulfamethazine (SMT) was tested using platinum (Pt), boron doped diamond (BDD), dimensionally stable anode (DSA, Ti/RuO_2-IrO_2) and graphite felt (GF). Comparison of the oxidation efficiencies of these anodes in the electro-Fenton process was performed at pH 3 and room temperature. High performance liquid chromatography (HPLC) and total organic carbon (TOC) were used to investigate the oxidative degradation kinetics of SMT and the extent of its mineralization in aqueous solution. The graphite felt was the most effective anode for oxidation of SMT at low current density but burned for long electrolysis times at high current densities. The absolute rate constant of the oxidation of SMT by hydroxyl radicals was determined by a competition kinetic method and found to be $2.9 \times 10^9\ M^{-1}\ s^{-1}$. BDD was found to be the best anode to mineralize SMT aqueous solutions, reaching almost total mineralization (98.5%). Determination of released inorganic ions: SO_4^{2-}, NO_3^-, and NH_4^+ gave additional evidences for the complete mineralization of SMT.

1. Introduction

The development of chemical industries and the increasing use of chemicals in many areas have led over the years to the accumulation of large variety of chemical pollutants in the environment [1–6]. Most of these chemicals are very stable and/or hardly degradable in the environment; they can migrate over very long distances from the place of their emission. Many of these substances represent adverse effects on living beings including humans [7–9]. The use of pesticides in agriculture, of dyes in textile industry, of pharmaceuticals in human and veterinary medicine and discharge of industrial wastewaters in natural water bodies, are some of the human activities that represent a permanent risk of environmental contamination and as consequence a threat for living beings. Therefore the treatment of wastewater before their injection in the natural water stream is important for sustainable environment. Conventional treatment technologies such as physicochemical (adsorption [10] or membrane filtration [11]) or microbiological [12,13] methods are not effective enough for the destruction of persistent organic pollutants. On the contrary, advanced oxidation processes (AOPs) [14–18] are effective and reliable for water remediation yielding almost complete mineralization of toxic or recalcitrant organic pollutants. These methods are based on the in situ production of highly reactive species, the hydroxyl radicals (•OH) which react unselectively with organic matter unto its total or quasi-total mineralization [19–21].

Among AOPs, electrochemical advanced oxidation processes (EAOPs) have received an increasing attention because of their efficiency in the destruction of toxic/persistent organic pollutants, environmental safety and computability and versatility [22–25]. One of the most popular EAOPs is the electro-Fenton process in which •OH are produced electrocatalytically through the Fenton Reaction (1); in this reaction H_2O_2 is electrogenerated from dissolved oxygen (Reaction (2)) and the Fe^{2+} (catalyst) is regenerated by electro-reduction of Fe^{3+} produced from reaction (1) [19,22,26,27].

$$H_2O_2 + Fe^{2+} \rightarrow Fe^{3+} + OH^- + {}^{\bullet}OH \quad (1)$$

$$O_2 + 2H^+ + 2e^- \rightarrow H_2O_2 \quad (2)$$

$$Fe^{3+} + e^- \rightarrow Fe^{2+} \quad (3)$$

* Corresponding author.
E-mail address: Mehmet.oturan@univ-paris-est.fr (M.A. Oturan).

http://dx.doi.org/10.1016/j.apcatb.2016.06.035
0926-3373/

Once produced in the solution (Reaction (1)), OH react very fast with organic pollutants leading to their oxidation unto complete mineralization (Reactions (4a) and (4b)).

$$\text{Organicpollutants} + {}^{\bullet}\text{OH} \rightarrow \text{oxidationintermediates} \quad (4a)$$

$$\text{Intermediates} + \text{OH} \rightarrow\rightarrow\rightarrow \text{CO}_2 + \text{H}_2\text{O} + \text{inorganicions} \quad (4b)$$

The Electro-Fenton process presents several advantages compared to the classical Fenton's system such as (i) in-site production of H_2O_2 that avoids the risks related to its transport, storage and handling, (ii) high oxidation/mineralization efficiency of organics due to the continuous electro-generation of the catalyst (Fe^2), (iii) easy control of the degradation kinetics, (iv) nonuse of harmful of chemical reagents and absence of formation of process sludge, and (iv) feasibility of total mineralization by optimizing the operating parameters [19,28–30].

The effectiveness of the electro-Fenton depends on several parameters such as current density [31] solution pH [32], catalyst concentration [33], etc. Anode material (M) also plays a significant role on the process efficiency [30,33,34]; its contribution becomes particularly important with high O_2 evolution overpotential materials [35–39]. Indeed, the use of such anodes allow to generate supplementary hydroxyl radical (M(•OH)) on their surface, from the oxidation of water, according to Reaction (5a) [30,40–42] which in turn enhances the degradation of organics (Reaction (5b)).

$$\text{M} + \text{H}_2\text{O} \rightarrow \text{M}({}^{\bullet}\text{OH}) + \text{H}^+ + \text{e}^- \quad (5a)$$

$$\text{M}({}^{\bullet}\text{OH}) + \text{organics} \rightarrow\rightarrow\rightarrow \text{M} + \text{CO}_2 + \text{H}_2\text{O} + \text{inorganicions} \quad (5b)$$

The aforementioned reactions highlights the electrocatalytic behavior of the process both in solution (electrogeneration of Fe^{2+} (Eq. (3)) to catalyze Fenton reaction (Eq. (1))) and at the anode (reconstitution of anode surface (Eq. (5b))). In addition to the in situ electrogeneration of H_2O_2 (Eq. (2)), the electrocatalysis constitutes a significant advantage for process efficiency and operation cost, making electro-Fenton a most advantageous and eco-friendly process compared to other AOPs such as classical Fenton system or photo-Fenton process.

There are only few papers reporting a systematic investigation on the effect of anode materials in the electro-Fenton process [30,43]. Most of these reports focused on a comparative study between Pt and boron doped diamond (BDD) anodes. We recently published a study on the effect of different anodes in oxidation of the antibiotic amoxicillin by the electro-Fenton process [36]; however this study focused on the development of a kinetic model based on mass transfer. Therefore a systematic work focused on the overall effect of anode material in the electro-Fenton process is important. Accordingly we conducted a comparative study on four different anode materials commonly used in electro-oxidation: Pt, BDD, DSA (Ti/RuO_2-IrO_2) and graphite felt (GF). As cathode material we have used the GF, the classical cathode of electro-Fenton process. The sulfamethazine (SMT), one of the most commonly used antibiotics from the 'sulphonamides' family, was selected as model pollutant because of its occurrence in natural water stream [1,44], and its adverse effects on living being such as: toxic effects to daphnia magna [8], fertility effects in mice [45] and thyroid hormone homeostasis in rats [46]. The performance of different anodes in the removal of SMT from water during an electro-Fenton process was assessed using the following parameters: (i) decay kinetics of the SMT concentration, (ii) total organic carbon (TOC) removal rate, (iii) concentration of released of inorganic ions during the treatment.

2. Experimental

2.1. Chemicals

Sulfamethazine (SMT) (4-amino-*N*-(4,6-dimethylpyrimidin-2-yl) benzenesulfonamide), $C_{12}H_{14}N_4O_2S$, was a sigma Aldrich product (≥99% purity) and was used without further purification. Methanol and phosphoric acid used in preparation of HPLC eluents, and Na_2SO_4 (>99% purity) as supporting electrolyte were from Sigma-Aldrich and Acros. HPLC eluents and SMT working solutions were prepared with ultra-pure water obtained from a Millipore Milli-Q system with resistivity >18 MΩ cm at room temperature. Potassium hydrogen phthalate (99.5%) used for TOC calibration was purchased from Shimadzu, France.

2.2. Electrolytic system

The electro-Fenton experiments were carried out in an open electrolytic cell containing a GF cathode of dimensions 17.5 cm × 5 cm × 0.5 cm and the tested anode of 24 cm^2 surface area. GF cathode was purchased from Carbone-Lorraine (France), whereas anodes were provided: Pt from Goodfellow (Lille, France) (France), Ti/RuO_2-IrO_2 (DSA) from Baoji Xinyu GuangJiDian Limited Liability Company (China), and Boron-Doped Diamond (BDD) from CONDIAS GmbH, (Germany). The electrolysis of SMT solutions were performed with a Hameg HM8040 triple power supply at constant current density, in a non-divided cylindrical glass cell of 300 mL capacity. Homogenization of the electrolysis solution was ensured with a magnetic stirring.

Oxidation of SMT was carried out at room temperature and pH 3which is suggested as optimal value for the electro-Fenton process [15,19]. The pH of solutions was adjusted with sulfuric or hydrochloric acids before starting electrolyses. The pH was measured with a CyberScan pH 1500 pH-meter from Eutech Instruments. The oxidation experiments were performed under current-controlled electrolysis conditions, at various constant current densities ranged from 2.08 to 20.83 mA cm^{-2}. Experiments for mineralization of SMT solutions were conducted at constant current density values ranging from 4.81 to 41.66 mA cm^{-2}, except for GF anode for which current of 2.08 and 4.16 mA cm^{-2} were applied. Aqueous solutions containing 0.2 mM (28.8 mg L^{-1}) SMT and 50 mM Na_2SO_4 were used for different trials. Samples were withdrawn during electrolysis at pre-set time intervals in order to assess the concentration decay of SMT, carboxylic acids evolution, inorganic ions released (due to the presence of heteroatoms S and N in the SMT structure) as well as TOC removal degree of treated solutions.

2.3. Analytical procedures

Although the concentration of SMT in natural water and soil was found at concentrations until 160 μg L^{-1} [1,44], the experiments were carried out with significantly higher concentration (0.2 mM) of SMT for the following reasons: (i) to facilitate the kinetic studies, (ii) to allow easy measurement of formed carboxylic acids and released inorganic ions and (iii) to highlight the capacity of the process to treat high concentrations present in the wastewater of hospitals, and production plants.

The samples were quenched, immediately after withdrawing, by Na_2SO_3 (100 μL of 50 mM Na_2SO_3 solution added to 1 mL of sample) to eliminate the residual H_2O_2. This residual H_2O_2 can be embarrassing in particular during toxicity measurements since it is toxic to *V. fischeri* bacteria.

Time course of SMT concentration during its oxidation was followed by reversed phase HPLC using a Merck Lachrom liquid chromatograph equipped with a quaternary pump L-7100, fitted

with a Purospher RP 18, 5 μm, 25 cm × 4.6 mm (id) column at 40 °C, and coupled with a L-7455 photodiode array detector selected at optimum wave length of 244 nm. The analysis of SMT decay was carried out isocratically with a mobile phase composed of 1% H_3PO_4 solution/methanol (90:10, v/v) mixture. A flow rate of 0.8 mL min^{-1} was always used. SMT showed a well-defined peak at retention time of 13.8 min under these conditions. Samples of 20 μL were injected into the HPLC and measurements were controlled through EZ-Chrom Elite 3.1 software.

The detection and evolution of carboxylic acids was followed by ion exclusion chromatography. An HPLC chromatograph equipped with pomp Alltech (Model 426) and a column Supelcogel H, 25 cm × 4.6 mm coupled to a detector Dionex AD20 was used. The eluent was a solution of sulfuric acid 9 mM. Flow rate was adjusted to 0.25 mL min^{-1}. Detection wave length for carboxylic acids was 220 nm and measures were done at 30 °C. The system is connected with an acquisition and data treatment unit commanded by analytical Chromeleon SE software.

Inorganic ions SO_4^{2-}, NO_3^- and NH_4^+ released in the solution from the degradation of SMT molecule were analyzed by ion chromatography. The ion chromatograph was a system Dionex ICS-1000. The data acquisition was done by Chromeleon software. This system is equipped either with a column cationic (CS12A) or anionic (AS4A-SC) of 4 mm diameter and 25 cm length coupled with a conductimetric detector DS6. In the case of cation detection the mobile phase was 9 mM sulfuric acid with the flow rate of 1 mL min^{-1}. The applied current in the suppressor SRS (Self Regenerating Suppressor) needed to prevent the influence of the eluent ions in the detector signal was 30 mA. For anions measurements the mobile phase contained 1.8 mM Na_2CO_3 and 1.7 mM $NaHCO_3$. The flow rate was fixed to 2 mL min^{-1}. The suppressor current was 30 mA.

In the case of SO_4^{2-} analysis by ionic chromatography, Na_2SO_4 was replaced by NaCl and $FeSO_4$ by $FeCl_3$ in order to avoid the SO_4^{2-} interference coming from the supporting electrolyte. Similarly for the analysis of NH_4^+, K_2SO_4 was used instead of Na_2SO_4 as the retention times of NH_4^+ and Na^+ are close and some possible overleap of NH_4^+ peak by that of Na^+ peak is possible because of the high concentration of the Na^+ of the supporting electrolyte.

The mineralization extent of electrolyzed solutions was assessed during the electro-Fenton treatment of SMT from the abatement of their TOC, determined on a Shimadzu TOC-V_{CSH} analyser according to the thermal catalytic oxidation method. The carrier gas was oxygen with a flow rate of 150 mL min^{-1}. The temperature in the oven was 680 °C. Platinum was used as catalyst in order to carry out the total combustion reaction at this temperature. Calibration of the analyser was done with potassium hydrogen phthalate standards.

3. Results and discussion

3.1. Kinetics of SMT degradation

The kinetics of oxidative degradation of organic pollutants in EF process is mainly governed by the generation rate of H_2O_2 and the nature of the anode. The former parameter controls the rate of the Fenton reaction and consequently the rate of formation of homogeneous OH while the second controls the amount and activity of heterogeneous M(•OH). The concentration of externally added catalyst (Fe^{2+}) reaches quickly a steady state value thanks to the large surface area of the graphite cathode and fast reduction of Fe^{3+} [47]. However, the optimal formation rate of H_2O_2 depends on the applied current and cathode material [48]. It increases with increasing applied current density up to an optimal value. Further increase in the current can be detrimental to formation of H_2O_2 because of promotion of 4-e^- reduction of O_2 leading to the formation H_2O as side reaction [22]. Therefore the applied current density is a main parameter in electro-Fenton process.

Fig. 1 shows the effect of current density on the oxidative degradation kinetics of SMT with a Pt anode during electro-Fenton (a) and anodic oxidation (b) processes. The applied current density increased from 4.16 to 12.50 mA cm^{-2} resulting, in both cases, in enhanced oxidation rates: the higher the applied current density the higher the decay in SMT concentration. This enhanced degradation kinetics of SMT is due to higher electrochemical hydrogen peroxide production (Reaction (2)) and catalyst (Fe^{2+}) regeneration (Reaction (3)) resulting in a higher concentration of homogeneous •OH in the solution bulk from Reaction (1). In addition, the increased current density leads to an enhanced production of Pt(•OH) on the anode surface [19]. Consequently, the higher production rate of hydroxyl radicals leads to a higher oxidation rate of SMT; however, the results of Fig. 1a also show that further increase in current density does not provides any significant improvement in the SMT decay kinetics. For instance, when applying 16.66 or 20.83 mA cm^{-2}, only a very small increase of the degradation rate is obtained, indicating that the current density of 12.50 mA cm^{-2} can be considered as the optimal value for SMT oxidation under the operating conditions of Fig. 1a. This results can be explained by an enhanced rate of the side reactions which compete with the oxidative degradation SMT. The most important of these side reactions are: (i) evolution of H_2 (Reaction (6)) at the cathode which competes with the formation of H_2O_2 and (ii) evolution of O_2 (Reactions (7) and (8)) at the anode which competes with the production of M(•OH) [19,22].

$$2H^+ + 2e^- \rightarrow H_2 \quad (6)$$

$$2H_2O \rightarrow O_2 + 4H^+ + 4e^- \quad (7)$$

$$2M(^\bullet OH) \rightarrow 2M + O_2 + 2H^+ + 2e^- \quad (8)$$

The contribution of the anodic oxidation of SMT (with a Pt anode) on the overall process is shown in Fig. 1b for two current densities; the experiments were performed without adding the catalyst Fe^{2+}. Significantly longer treatment times are needed to reach complete oxidation of SMT indicating that its oxidation by Pt(•OH) is less efficient than the oxidation by homogeneous •OH. For instance even after 90 min of electrolysis at 500 mA, in absence of Fe^{2+}, there are still some traces of SMT remaining in the solution, while complete oxidation required less than 10 min in the case of the electro-Fenton process (in the presence of Fe^{2+}).

The oxidation performance of the DSA anode was then tested in a DSA/GF cell under the same operating conditions (Fig. 2). The rate of oxidation increases with the current densities unto a limiting value of 16.66 mA cm^{-2}. The degradation efficiency is slightly lower than that of a Pt/GF cell: 20 and 70 min are needed for complete degradation of SMT with current densities of 20.83 and 4.16 mA cm^{-2}, respectively, versus 10 and 60 min in the case of Pt anode. This reflects slower oxidation kinetics and inferior oxidation capacities of the DSA anode compared to the Pt anode. This difference is probably related to the adsorption characteristics: DSA(•OH) are more strongly adsorbed on the anode surface than Pt(•OH) and consequently less available for oxidation of SMT.

Fig. 3 shows the impact of different current densities on the decay of the SMT concentration during its electro-oxidation in a BDD/GF cell both by electro-Fenton and anodic oxidation processes. The decay of the SMT concentration with time is always exponential pointing out the pseudo-first order kinetics for the whole range of applied currents. The rate of the SMT oxidation reaction increases as for Pt/GF and DSA/GF cells, unto the optimal current density of about 12.50 mA cm^{-2} but slightly faster with BDD/GF than with the former anodes. This better performance of BDD anode in oxidation of SMT can be explained by its higher O_2 evolution overpotential promoting the formation of high amount of BDD(•OH) [22,40].

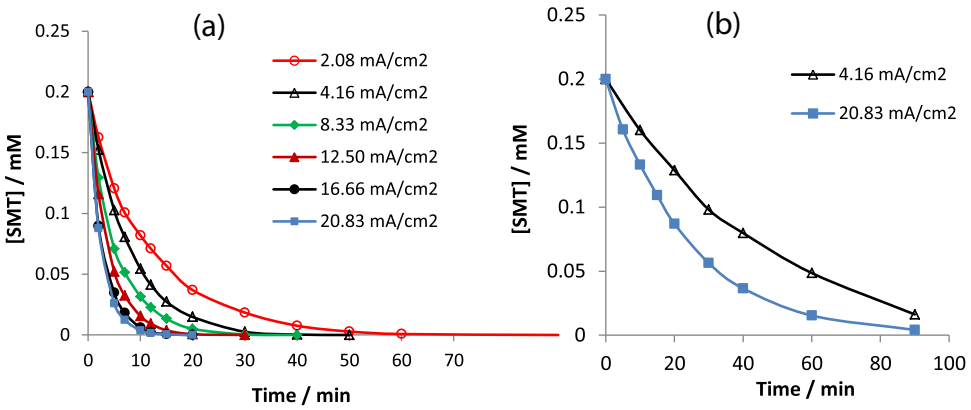

Fig. 1. The effect of current density on the kinetics of degradation of SMT using the Pt/GF electrode couple. (a) electro-Fenton and (b) anodic oxidation. V_s = 300 mL, pH = 3, $[Na_2SO_4]$ = 50 mM, $[Fe^{2+}]$ = 0.2 mM for electro-Fenton and 0.0 mM for anodic oxidation.

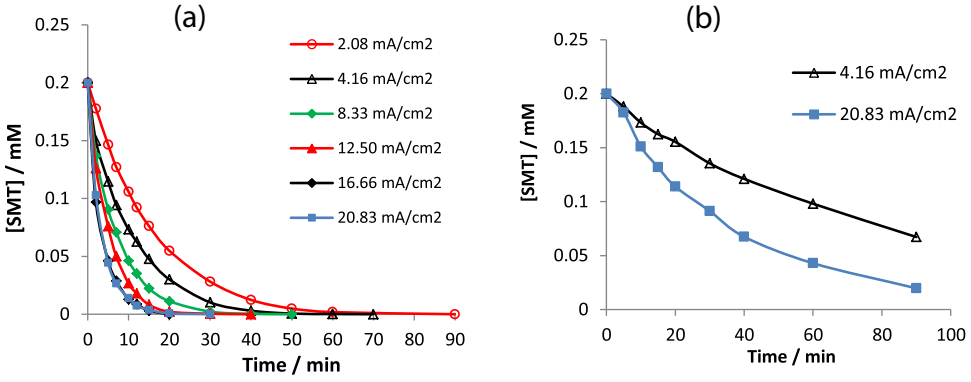

Fig. 2. The effect of current density on the kinetics of degradation of SMT using the DSA/GF electrode couple: (a) electro-Fenton, (b) anodic oxidation. V_s = 300 mL, pH = 3, $[Na_2SO_4]$ = 50 mM, $[Fe^{2+}]$ = 0.2 mM (electro-Fenton only).

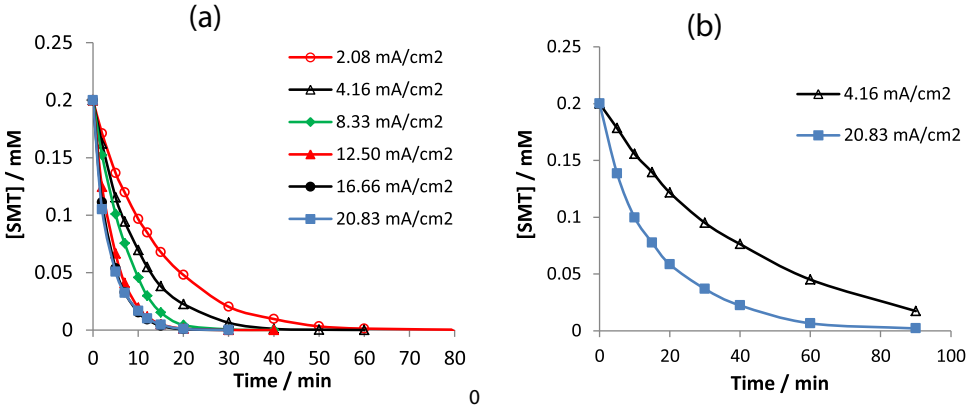

Fig. 3. The effect of current density on the kinetics of degradation of SMT using the BDD/GF electrode couple: (a) electro-Fenton, (b) anodic oxidation. V_s = 300 mL, pH = 3, $[Na_2SO_4]$ = 50 mM, $[Fe^{2+}]$ = 0.2 mM (only for electro-Fenton).

The results obtained with GF as anode and cathode (GF/GF cell) are depicted in Fig. 4; they show a very different behavior. Fig. 4a shows that, in the electro-Fenton process, the SMT concentration decay is very fast in comparison with the preceding cells. For instance, the time required for total disappearance of SMT (15 min) is 3–4 time shorter than with Pt, DSA or BDD anodes, for which this performance is attained only for the optimal current density (12.50–16.66 mA cm^{-2}) values. For 12.50–20.83 mA cm^{-2} current densities, the kinetics curves exhibit similar shapes for SMT disappearance. The anode underwent combustion reaction at high current density values. Therefore, the effect of increasing current density is limited by the loss of electrode surface, due to its partial combustion. The same behavior is also observed in the case of the anodic oxidation highlighting the significant performance of the GF anode in the oxidation rate of SMT.

Overall, Figs. 1–4 evidence the predominant role of homogeneousOH in oxidation of organic during electro-Fenton process. The contribution of M(OH) remains limited, particularly in the case of Pt and DSA anodes, due to the limiting mass transfer from the anode to the solution since the oxidation reaction takes place in the vicinity of the anode surface.

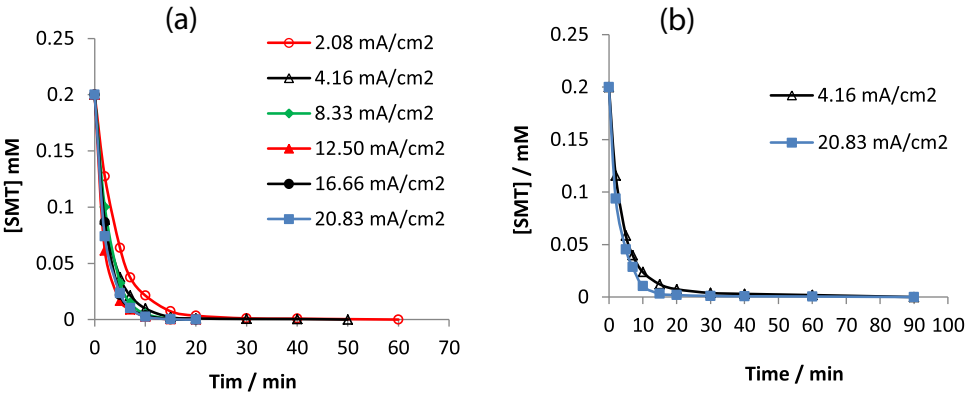

Fig. 4. The effect of current density on the kinetics of degradation of SMT using the GF/GF electrode couple: (a) electro-Fenton, (b) anodic oxidation V_s = 300 mL, pH = 3, $[Na_2SO_4]$ = 50 mM, $[Fe^{2+}]$ = 0.2 mM (for electro-Fenton only). Current density calculated from the geometrical surface of the anode as for other anodes.

Table 1
Apparent rate constants (k_{app} in min^{-1}) as a function of the anode material and the current density for electro-Fenton process with graphite felt cathode.

Anode		k_{app} (min^{-1})		
I ($mA\,cm^{-2}$)	Pt	DSA	BDD	GF
2.08	0.08	0.06	0.07	0.22
4.16	0.15	0.09	0.12	0.31
8.32	0.19	0.14	0.18	0.37
12.50	0.27	0.20	0.24	0.44
16.66	0.37	0.27	0.27	0.43
20.83	0.40	0.27	0.25	0.43

Table 2
Apparent rate constants as a function of the anode material and the current density for the anodic oxidation process. The cathode is graphite felt.

Anode		k_{app} (min^{-1})		
I ($mA\,cm^{-2}$)	Pt	DSA	BDD	GF
2.08	0.02	0.01	0.02	0.22
4.16	0.04	0.02	0.6	0.29

Hydroxyl radicals are known for their extreme reactivity and non-selectivity towards organic molecules. Once created in the solution they react immediately with whatever molecule that they come across first. This very short life time prevents them from being accumulated in the medium. For a constant current density, a constant rate of •OH production is obtained, therefore their concentration reaches quickly a quasi-stationary state; whereby a pseudo-first order kinetics can be established for the oxidation reaction of organics. The experimental data for concentration of SMT vs electrolysis time, permit to calculate the apparent rate constants from the semi logarithmic plots ln $(C_0/C) = f(t)$; their values are given in Table 1. According to the apparent rate constants (k_{app}) obtained for oxidation SMT by hydroxyl radicals, DSA anode showed the lowest efficiency followed by BDD and Pt; GF anode exhibiting significantly higher k_{app} values. In all cases the SMT degradation rate increases with the current until an optimal current density of about 12.50–16.66 $mA\,cm^{-2}$. Concerning the optimal current density, a characteristic behavior is observed for the GF anode: when the current density increases from 2.08 to 12.50 $mA\,cm^{-2}$, the k_{app} increases less for GF than for the other anodes and the kinetic curves stay closer to each other. This behavior can be explained by partial combustion of the anode material enhanced by increasing applied current values. Therefore the increase in k_{app} brought by the increasing current would be partially cancelled by the partial oxidation of the anode leading to k_{app} increasing slower with the current density.

The k_{app} values for the oxidative degradation of SMT by anodic oxidation process are given in Table 2. There is a clear difference between k_{app} values for Pt and BDD anodes in the anodic oxidation and electro-Fenton processes. Unlike in the electro-Fenton process, the BDD anode oxidizes SMT faster than the Pt anode in anodic oxidation. This trend is normally expected for the BDD anode that presents a higher overpotential for O_2 evolution reaction (OER) than Pt, which permits to obtain high concentration of hydroxyl radicals. In addition, the high oxidation performance of the BDD anode is also related to the fact that BDD(•OH) are physisorbed on the anode surface and readily available for oxidation of organics in contrast to Pt(•OH) that are chemisorbed. This difference appears very weakly in electro-Fenton because the oxidation process occurs mainly through homogeneous •OH (Reaction (1)).

The slight difference between k_{app} for Pt/GF, BDD/GF and DSA/GF cells in the electro-Fenton process can be explained overwhelmingly by the effect of •OH generated in high amount in the bulk of solution; they quickly destroy organics with high oxidation rate constants. Therefore part of the anode effect is hidden by the dominating electro-Fenton action, in particular at high applied current densities.

The significantly better performance (for equal apparent surfaces) of the GF/GF cell is the result of the much larger specific surface area (0.7 $m^2\,g^{-1}$) of the GF material owing to its high porosity, specific area and 3D geometry (other anodes having a specific surface area equal to their apparent surface area). Therefore this anode permits to generate high amounts of hydroxyl radicals that increase the degradation of SMT in both processes. This substantial contribution is clearly pointed out in Fig. 4 where the decay kinetics of SMT during anodic oxidation is close to that obtained in the electro-Fenton. These results highlight that the AO process dominates over generation of •OH in solution by Reaction (1). However, the GF anode provides a good oxidation efficiency at low current densities but it is not suitable for high currents densities that lead to its combustion.

In order to determine the absolute rate constant of the oxidation of SMT by hydroxyl radicals, we have used the method of competition kinetics [15,28,49]. The experiments were done in the Pt/GF cell at current density of 2.08 $mA\,cm^{-2}$ in order to avoid side reactions. This method consists in the simultaneous degradation of the compound of concern and a standard compound (competitor) with a well-known absolute rate constant of its reaction with hydroxyl radicals. Therefore p-hydroxybenzoic acid (p-HBA) acid ($k_{pAHB} = 2.19 \times 10^9\ M^{-1}\,s^{-1}$) [50] was used as standard competitor for the determination of the absolute rate constant of SMT oxidation by hydroxyl radicals. The concentration decay of SMT and p-HBA was followed and measured by HPLC analysis on a short treatment time. The slope of the linear curve of Fig. 5 allowed

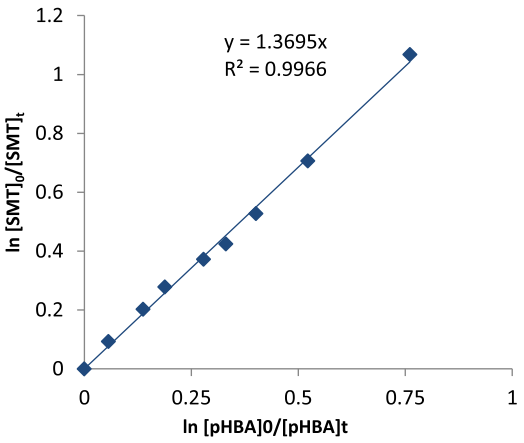

Fig. 5. Kinetic analysis for the absolute reaction rate constant for oxidation of SMT with OH. Electro-Fenton cell: Pt/GF, V_s = 300 mL, $[Fe^{2+}]$ = 0.2 mM, $[Na_2SO_4]$ = 50 mM, I = 2.08 mA cm^{-2}, pH = 3.

determination of the rate constant k_{SMT} to be 2.9×10^9 M^{-1} s^{-1}. We did not find already reported k_{SMT} value for comparison but this value is in line with the absolute rate constants for the •OH hydroxylation of several pharmaceuticals and aromatic organic compounds [15,19].

3.2. Comparison of the mineralization efficiency

The total removal of organic pollutants from treated water is of high importance because they have various adverse effects on the environment. The oxidation or partial mineralization of organic pollutants during an AOP treatment can lead to the formation of more toxic intermediates than the initial pollutant [51–53]. Accordingly the oxidative degradation of the persistent/toxic chemicals must continue unto the quasi-complete mineralization of the treated solution. The toxicity being generally linked to aromatic/cyclic moieties of organics, the oxidative cleavage of these rings is essential for removal of toxicity. The complete mineralization of organics is a complicated oxidation process and needs significantly long treatment times to be achieved. The electro-Fenton process is one of the most powerful methods to mineralize the organic matter in aqueous solution achieving high TOC removal efficiency. Furthermore the extent of the mineralization degree of this technology depends on several parameters, one of the most crucial being the nature of the anode material used.

As it can be seen in Fig. 6a, the mineralization of SMT is improved by an increased current density in the Pt/GF cell; up to 20.88 mA for a maximum value of the TOC removal. Further increase in current density does not enhance the mineralization efficiency. In contrast, currents higher than 20.83 mA cm^{-2} lead to slower TOC removal kinetics: for 29.16 and 41.66 mA cm^{-2}, TOC removal curves have a lower slope than that of 12.50 mA cm^{-2}, leading to poorer mineralization kinetics towards the end of treatment. The decrease of the mineralization yield is related to the increased efficiency of side Reactions (6)–(8) that hinder the generation or favor the consumption of OH/M(•OH). Fig. 6 also shows a very sharp decay of TOC during the first part of electrolysis (until 4 h) followed by a much slower rate over longer treatment times. This behavior is reported in the literature [19,22] and can be explained by the formation of more recalcitrant organic compounds such as short–chain carboxylic acids or their iron(III) complexes that are relatively resistant to OH and accumulate in the solution. The reinforcement of some parasitic reactions because of the low concentration of organic matter in the medium can also explain these slower kinetics; the most important of these reactions being the consumption of OH by Fe^{2+} ions; the rate constant of this reaction ($k = 3.2 \times 10^8$ M s^{-1}) and that of the oxidation of carboxylic acids are of the same order of magnitude.

By comparison, Fig. 6b shows the mineralization curves for the anodic oxidation; it indicates clearly that the TOC abatement is very small compared with the electro-Fenton even for high currents. For instance, TOC removal yield was 92.2% in electro-Fenton with the optimal current density of 20.83 mA cm^{-2} at 8 h, whereas only 41% TOC removal could be achieved at the same conditions with anodic oxidation.

The experiments with the DSA/GF system revealed a poorer TOC abatement than with Pt/GF cell, reaching 71.3% at 8 h treatment. Even if the TOC decay kinetics is improved by increasing current density (Fig. 7a) the TOC removal curves for 4.16, 20.83 mA cm^{-2} are closer to each other than those of Pt/GF cell. This means that the optimal current is attained at lower values for the DSA; it indicates that during the SMT oxidation the OER is more dominating on a DSA than on a Pt anode. However the anodic oxidation of SMT with a DSA anode exhibits a very low efficiency regardless applied current density (Fig. 7b). Therefore, the relatively high mineralization rates obtained in electro-Fenton treatment can be attributed to the homogeneous OH generated in the bulk (Reaction (1)): they are able to oxidize quickly SMT without significant contribution of DSA(OH).

With the BDD anode, the effect of current density on the mineralization of SMT is given in Fig. 8, where a new trend is observed. Unlike with the preceding anodes, the range of current densities for the mineralization of organics is extended in the case of BDD anode. For Pt and DSA anodes the optimal current density was

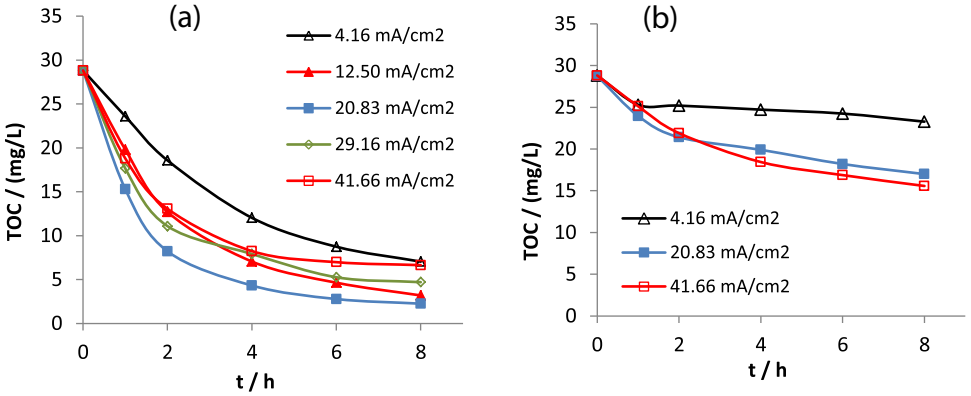

Fig. 6. Effect of applied current density on the extent of TOC removal of SMT aqueous solution in the cell Pt/GF during (a) electro-Fenton and (b) anodic oxidation. V_s = 300 mL, pH = 3, $[Na_2SO_4]$ = 50, mM $[Fe^{2+}]$ = 0.2 mM (for electro-Fenton).

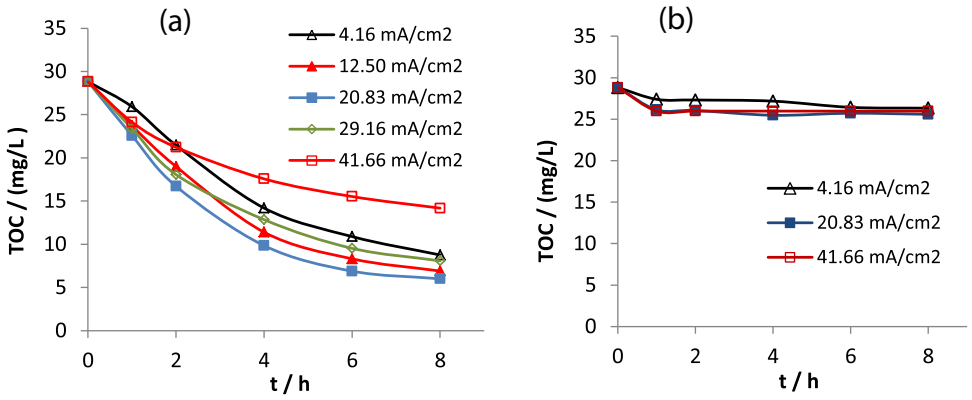

Fig. 7. Effect of current density on the extent of TOC removal in the cell DSA/GF. (a) electro-Fenton, V_s = 300 mL, pH = 3, $[Fe^{2+}]$ = 0.2 mM, $[Na_2SO_4]$ = 50 mM (b) Anodic mineralization of SMT: V_s = 300 mL, pH = 3, $[Na_2SO_4]$ = 50 mM.

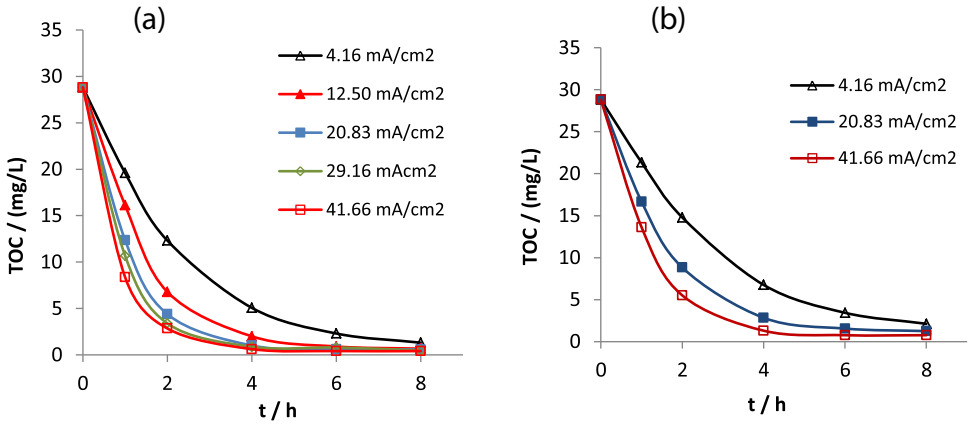

Fig. 8. Effect of current density on the extent of TOC removal in the cell BDD/GF during mineralization of SMT aqueous solution by (a) electro-Fenton and (b) anodic oxidation. V_s = 300 mL, pH = 3, $[Fe^{2+}]$ = 0.2 mM (for electro-Fenton only), $[Na_2SO_4]$ = 50 mM.

20.83 mA cm^{-2}, whereas for BDD anode, the mineralization efficiency can be improved up to 41.66 mA cm^{-2}. This is possible due to the high overpotential of OER on BDD which enables the generation of high amount of BDD(•OH) and their accumulation on its surface. Comparing the TOC abatement between electro-Fenton and anodic oxidation a quite small difference is observed; this results from the predominant role of BDD(OH) in the mineralization process compared to that of homogeneous OH generated in the bulk solution.

The mineralization of SMT in solution with a GF anode was conducted only at low current densities of 2.08 and 4.16 mA cm^{-2} because this anode burns at higher current densities at longer electrolysis time (Fig. 9). The mineralization rate is relatively good at short treatment times (until 4 h) being slightly lower than BDD but significantly better than with Pt or DSA anodes. For 4.16 mA cm^{-2} current density, the TOC decays quickly until 4 h electrolysis, it is almost constant up to 6 h and finally reaches a lower value at 8 h than that of 6 h. This result is somewhat surprising, but considering the results obtained during SMT oxidation experiments, the increased carbon in the solution may be attributed to the burning of GF during longer electrolysis. The burning of GF results in heating the system, water vaporization, decrease of the volume and finally in an increased total carbon concentration. Anyways GF can be considered as an interesting anode material that provides very good oxidative degradation and relatively good TOC removal values at low current densities resulting in low energy consumption.

Table 3 summarizes the mineralization of SMT with different anodes. As mentioned above the mineralization efficiency of

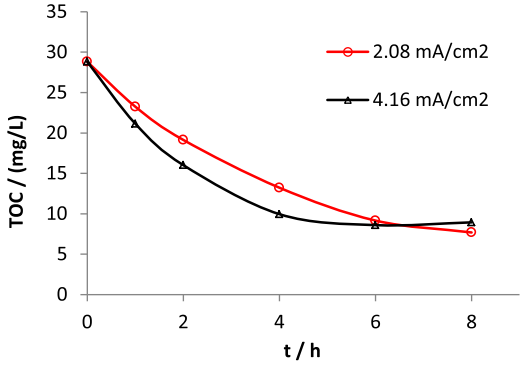

Fig. 9. Effect of current density on the extent of TOC removal in the GF/GF cell during electro-Fenton process. V_s = 300 mL, pH = 3, $[Fe^{2+}]$ = 0.2 mM (in electro-Fenton), $[Na_2SO_4]$ = 50 mM.

Table. 3
TOC removal percentages during electro-Fenton treatment of 0.2 mM SMT solution as function of the anode material and the current density at treatment times of 2 and 6 h.

Anode	TOC removal (%) at 2/6 h			
I (mA cm^{-2})	Pt	DSA	BDD	GF
2.08				33.6/68.2
4.16	35.5/69.6	25.5/62.2	57.2/91.9	44.4/70.2
12.50	55.9/83.9	34.1/71.1	76.4/96.8	
20.83	41.5/90.3	41.9/76.1	84.7/96.9	
29.16	61.4/81.7	34.8/75.2	88.2/97.4	
41.66	54.7/75.8	26.3/46.1	90.1/98.5	

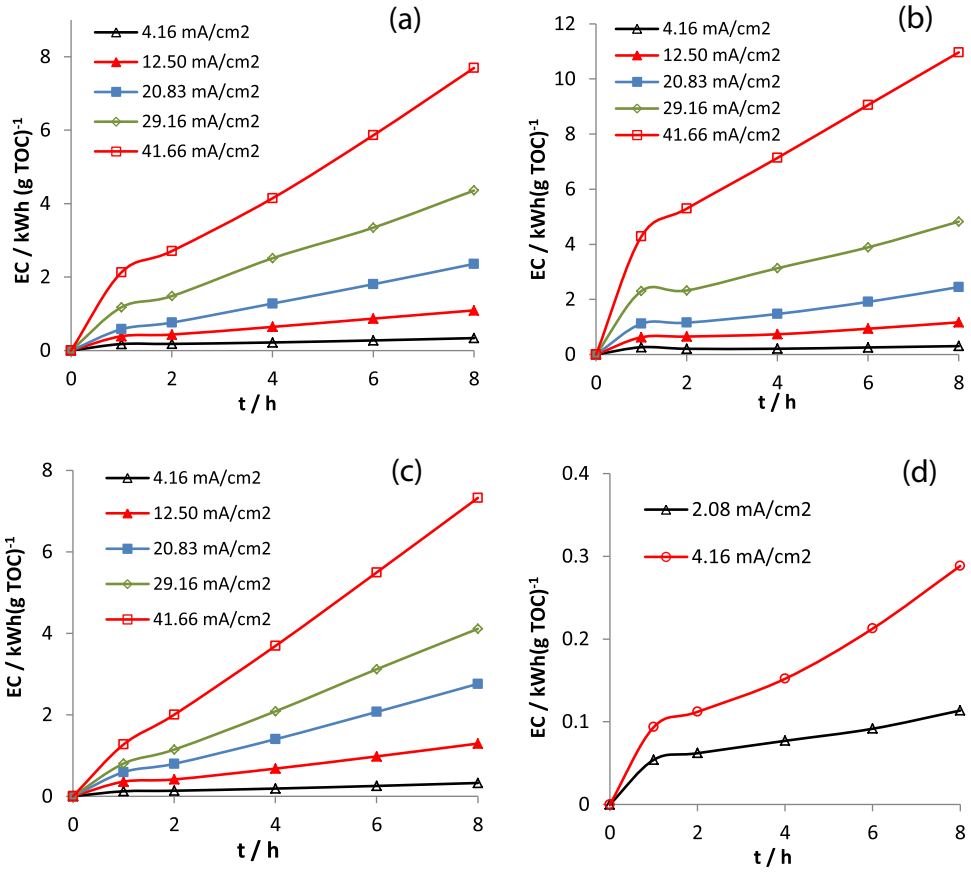

Fig. 10. Evolution of energy consumption (EC) in kWh per g TOC removed during electro-Fenton process with different anodes: (a) Pt, (b) DSA, (c) BDD and (d) GF, under conditions of Figs. 6–10.

anodes according to the TOC removal percentage (as mineralization efficiency) ranks as follows: BDD > Pt > DSA, whereas GF is only effective for low currents; the latter provides, at 50 mA, a mineralization efficiency close to that of Pt with 100 mA and clearly better than that of DSA anode.

These results highlight the very weak contribution of anodic oxidation to the mineralization efficiency in case of Pt and DSA anodes (Figs. 6 and 7), particularly at low current densities evidencing the prevailing effect of homogeneous OH in the mineralization process. Nevertheless the contribution of BDD(•OH) to the mineralization of SMT solutions is important (Fig. 8) due to its large mineralization power as already reported [19,22,43].

The outstanding oxidation capabilities of BDD comes, as stated before, from the generation of high amount of BDD(OH) which are weakly physisorbed and free to react with organics. In the case of DSA anode, the electronic structure permits higher oxidation states for iridium without notable formation of free radical. Thus Ir (IV) in IrO_2 oxidizes to Ir (VI) as IrO_3 (Reaction (9)) [54] and then iridium trioxide oxidizes the organic matter along a rather slow chemical reaction.

$$IrO_{2(s)} + H_2O \rightarrow IrO_{3(s)} + 2H^+ + 2e^- \quad (9)$$

At high current densities (or high potentials) the O_2 evolution rate from IrO_3 according to the Reaction (9) becomes faster than the SMT oxidation by IrO_3 lowering its oxidation efficiency. Higher oxidation states have also been proposed for Pt [39], but as oxygen evolution overpotential is higher than on DSA, small quantities of Pt(OH) are generated [40].

Another interesting point in the comparison of anodes is the electrical energy consumption (EC). This parameter is determined in term of kWh energy per g TOC removed during the mineralization experiments and calculated from the following equation.

$$\mathrm{EC}\left(\mathrm{kWh\ (kg\,TOC)^{-1}}\right) = \frac{E_{cell} I t}{(\Delta(\mathrm{COD})_t V_s} \quad (10)$$

where E_{cell} is the average cell voltag (V), I is the applied current (A), t is the electrolysis time (h), V_s is the solution volume (L) and $(\Delta\mathrm{TOC})_t$ is the TOC decay (g O_2 L^{-1}) at time t.

The results are depicted in Fig. 10 for the different anodes under study. The results clearly show that during the electro-Fenton process the applied current value is the most influencing parameter on EC, along with the electrolysis time. EC is particularly high in the case the DSA anode due to its lower mineralization capacity and particularly low for the GF anode at low current density. Pt and BDD anodes provide similar results; the relatively high difference of potential (V) developed by BDD anode is counterbalanced by its high mineralization power.

3.3. Determination and evolution of carboxylic acids during electro-Fenton treatment of SMT

The advanced oxidation of organic compounds is accompanied by the formation of intermediate products [51,55]. Short-chain carboxylic acids are the lowest molecular weight organic species formed before complete mineralization (i.e., transformation to CO_2, H_2O and inorganic) of organic pollutants during AOPs. Fig. 11 shows the formation and evolution of different carboxylic acids generated during the oxidative degradation of SMT with Pt, DSA and BDD anodes by electro-Fenton process. Five carboxylic acids, namely oxalic, glyoxylic, oxamic, formic and maleic acids were identified and quantified for Pt/GF, DSA/GF and BDD/GF cells with different

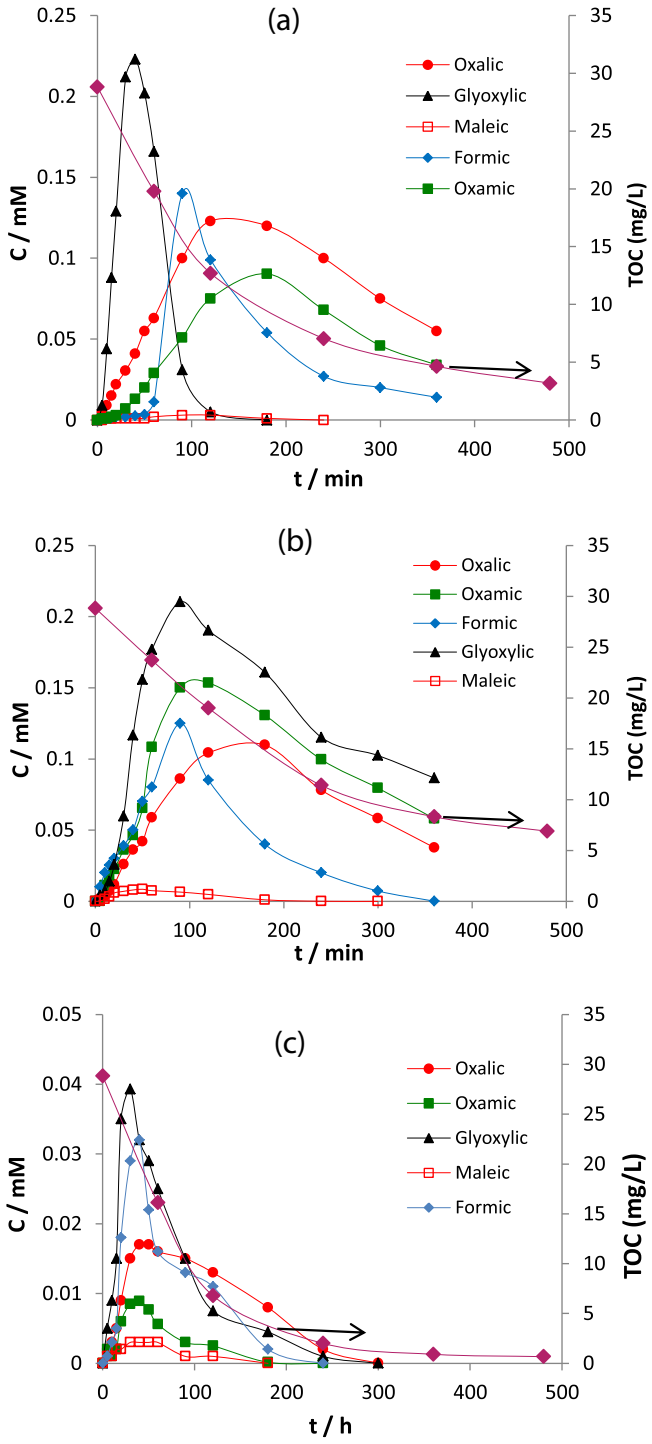

Fig. 11. Time course of carboxylic acids formed during electro-Fenton treatment of SMT with different electrolytic cells: (a) Pt/GF, (b) DSA/GF and (c) BDD/GF. V_s = 300 mL, [SMT] = 0.2 mM, $[Fe^{2+}]$ = 0.2 mM, $[Na_2SO_4]$ = 50 mM, I = 12.50 mA cm^{-2}, pH = 3. The pink curve (–♦–) show the decay of TOC during treatment.

accumulation trends as shown on Fig. 11. Malonic and pyruvic acids were detected at trace level. These acids are generated starting from the beginning of the electrolysis and accumulate in the medium up to maximum values; this maximum occurs at different times depending on the nature of the anode material. In particular, glyoxylic acid accumulates quickly at short electrolysis time reaching a maximum concentration at about 30, 50 and 90 min with BDD, Pt and DSA anodes, respectively. It is then rapidly mineralized in the BDD/GF cell (after about 1 h) while it remains in significant concentration even after 6 h electrolysis in the DSA/GF cell. Carboxylic acids are completely mineralized at 300 min when BDD is used as an anode whereas they remain at relatively high concentrations with Pt/GF and DSA/GF cells. The relatively high TOC value measured in the case of Pt/GF and DSA/GF cells at the end of treatment is mainly composed of short-chain carboxylic acids remaining in solution (Fig. 11a,b). These results point out again the outstanding mineralization capabilities of the BDD anode (Fig. 11c); the residual TOC remaining at the end of treatment is particularly low. This behavior is also reflected in mineralization kinetics as depicted in Figs. 6–8.

Table 4
TOC removal percentages during the anodic oxidation of 0.2 mM SMT solution as a function of anode material and current density.

Anode	TOC removal (%) at 2/6 h			
I (mA cm^{-2})	Pt	DSA	BDD	GF[1]
4.16	12.5/15.8	5.2/8.3	48.7/88.1	–
20.83	25.7/36.8	9.6/10.8	69.4/94.6	–
41.66	24.0/41.4	9.8/9.8	80.9/97.	–

[1] TOC could not be correctly measured because of carbon released from the cathode during long time electrolysis.

3.4. Evolution of inorganic ions during the mineralization of SMT

When the organic molecules contain heteroatoms in their structure, they are oxidized to inorganic ions released in the solution during mineralization process [15,19,56]. The release of inorganic ions constitutes another proof of mineralization of organics. SMT is a sulfonamide antibiotic which contains one S and 4 N in its initial structure. Consequently at least three inorganic ions: NO_3^-, NH_4^+ and SO_4^{2-} are expected in the electrolyzed solution (Table 4).

In the analysis of SO_4^{2-}, NaCl was used as a supporting electrolyte to avoid the interference of Na_2SO_4. The use of NaCl can modify slightly the concentration of the final nitrogen products. In fact, chloride ions can be oxidized at the anode (in particular with the BDD anode) to Cl_2 which reacts with water to form the $HClO/ClO^-$ couple [35] and [40]. These relatively weak oxidants can contribute to the mediated oxidation of some readily oxidizable organics but in general the mediated oxidation has no significant effect on the mineralization efficiency. Therefore the effect of mediated oxidation by active chlorine species was neglected in this study.

The evolution of these inorganic ions was analyzed in the different cells studied in this work by ion-exclusion chromatography during electro-Fenton treatment of 0.2 mM SMT and the results are presented in Fig. 12. The release of SO_4^{2-} is very fast and quantitative in all cases; the theoretical concentration of 0.2 mM is reached at about 30 min and remains constant along the treatment. This very rapid release of the quantitative SO_4^{2-} amount suggests that the SMT degradation starts mainly by sulfur extrusion.

The concentration of nitrogen ions evolves slowly except with the Pt anode for which the sum of NO_3^- and NH_4^+ represents 90% of the nitrogen theoretically expected for the complete mineralization of SMT (Fig. 12a); NO_2^- ion was not detected in the solution. At the beginning of the experiment, the concentration of NO_3^- increases slowly and accumulates at an increased rate during the 3 h treatment. NH_4^+ is released at relatively low concentration compared to NO_3^- with a continued increase up to 6 h. In the DSA/GF cell nitrogen is released as NO_3^- and NH_4^+ in low concentration as expected from the relatively low mineralization of SMT with this anode (Figs. 7 and 12 b). The sum of NO_3^- and NH_4^+ corresponds to 60% of the theoretical nitrogen. This poorer mass balance can be also explained in part by the presence of oxamic acid (Fig. 11b) in significant concentration but also by the formation and later strip-

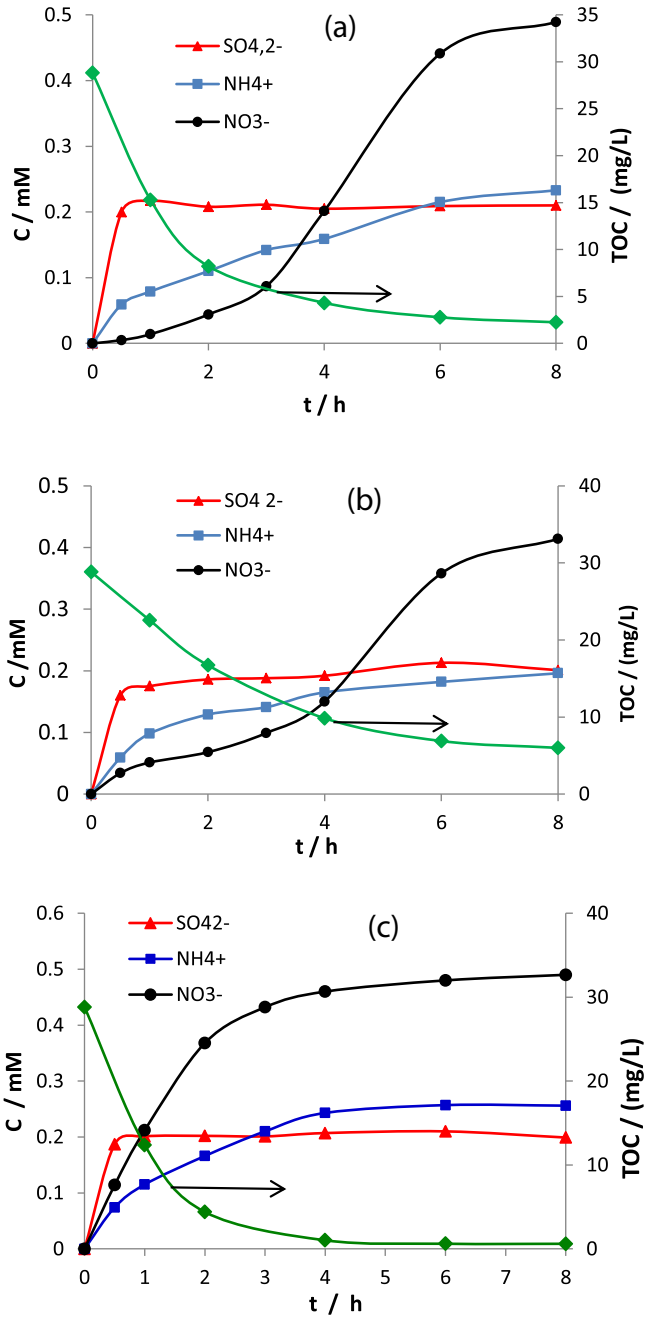

Fig. 12. Time course of inorganic ions formed during electro-Fenton treatment of SMT with electrolytic cells: (a) Pt/GF, (b) DSA/GF and (c) BDD/GF. For NO_3^-: V_s = 300 mL, $[SMT]_0$ = 0.2 mM, $[Fe^{2+}]$ = 0.2 mM, $[Na_2SO_4]$ = 50 mM, I = 20.83 mA cm^{-2}, pH = 3. For NH_4^+: V_s = 300 mL, [SMT] = 0.2 mM, $[Fe^{2+}]$ = 0.2 mM, $[K_2SO_4]$ = 50 mM, I = 20.83 mA cm^{-2}, pH = 3. For SO_4^{2-}: V_s = 300 mL, [SMT] = 0.2 mM, $[Fe^{2+}]$ = 0.2 mM, [NaCl] = 50 mM, I = 20.83 mA cm^{-2}, pH = 3. The green curve (–♦–) represents the evolution of solution TOC during treatment. (For interpretation of the references to colour in this figure legend, the reader is referred to the web version of this article.).

ping of ammonia to N_2 under the strongly alkaline conditions near the cathode surface [57,58]. With the BDD/GF cell the nitrogen ions concentration released (Fig. 12c) is less (63%) than that expected from the high TOC removal rate obtained with this cell. The NO_3^- and NH_4^+ ions are released quickly until 4 h according to the high mineralization kinetics (Fig. 12c) before reaching a plateau. Small amounts of nitrogen can also be present as oxamic acid. However the greatest part of the loss in the nitrogen balance can be related to formation of gaseous nitrogen compounds (N_2, N_2O_5...), in particular, at the BDD anode and also by the formation and stripping of ammonia to N_2 under the strongly alkaline conditions at the vicinity of the cathode surface.

4. Conclusions

The electro-Fenton efficiency effect of four anode materials (Pt, DSA, BDD and GF), has been investigated for the destruction of the antibiotic SMT –as a model pollutant. The kinetic study in terms of apparent rate constants revealed only small differences between the degradation efficiencies on Pt, DSA and BDD anodes; the highest degradation performance was measured for the GF anode at low current densities. A relatively high absolute rate constant ($k_{SMT} = 2.9 \times 10^9$ M^{-1} s^{-1}) for the oxidation of SMT by •OH was determined using competition kinetics method. Different mineralization performances were observed with the sequence BDD ≫ Pt > DSA. GF can be used only at low current densities (about of 50 mA) since it starts burning at higher currents. A very high mineralization efficiency (in terms of TOC removal) was obtained with a BDD anode in relation of its very high O_2 evolution overpotential and the weak adsorption of BDD(•OH). This behavior is also confirmed by the release of inorganic ions at almost the theoretically expected concentrations.

Acknowledgement

Flamur Sopaj acknowledges the embassy of France in Kosovo for the PhD scholarship granted by the French government, which enabled the realization of this work.

References

[1] K. Kümmerer, Antibiotics in the aquatic environment–a review–part I, Chemosphere 75 (2009) 417–434.
[2] S.K. Khetan, T.J. Collins, Human pharmaceuticals in the aquatic environment: a challenge to green chemistry, Chem. Rev. 107 (2007) 2319–2364.
[3] L. Feng, E.D. van Hullebusch, M.A. Rodrigo, G. Esposito, M.A. Oturan, Removal of residual anti-inflammatory and analgesic pharmaceuticals from aqueous systems by advanced oxidation processes. A review, Chem. Eng. J. 228 (2013) 944–964.
[4] S. Chiron, L. Comoretto, E. Rinaldi, V. Maurino, D. Vione, Pesticide by-products in the Rhone delta (Southern France). The case of 4-chloro-2-methylphenol and of its nitroderivative, Chemosphere 74 (2009) 599–604.
[5] L.R. Zimmerman, E.M. Thurman, K.C. Bastian, Detection of persistent organic pollutants in the Mississippi Delta using semipermeable membrane devices, Sci. Total Environ. 248 (2000) 169–179.
[6] S. Vasudevan, M.A. Oturan, Electrochemistry as cause and cure in water pollution. An overview, Environ. Chem. Lett. 12 (2014) 97–108.
[7] Q.Q. Li, A. Loganath, Y.S. Chong, J. Tan, J.P. Obbard, Persistent organic pollutants adverse health effects in humans, J. Toxicol. Environ. Heal A 69 (2006) 1987–2005.
[8] LHMLM Santos, A.N. Araujo, A. Fachini, A. Pena, C. -Delerue-Matos, M.C.B.S.M. Montenegro, Ecotoxicological aspects related to the presence of pharmaceuticals in the aquatic environment, J. Hazard. Mater. 175 (2010) 45–95.
[9] K. Fent, A. Weston, D. Caminada, Ecotoxicology of human pharmaceuticals, Aquat. Toxicol. 76 (2006) 122–159.
[10] S.-H. Lin, R.-S. Juang, Adsorption of phenol and its derivatives from water using synthetic resins and low-cost natural adsorbents: a review, J. Environ. Manage. 90 (2009) 1336–1349.
[11] A. Sonune, R. Ghate, Developments in wastewater treatment methods, Desalination 167 (2004) 55–63.
[12] F.P. Van der Zee, S. Villaverde, Combined anaerobic-aerobic treatment of azo dyes —a short review of bioreactor studies, Water Res. 39 (2005) 1425–1440.
[13] B. Demirel, O. Yenigun, T. Onay, Anaerobic treatment of dairy wastewater: a review, Process Biochem. 40 (2005) 2583–2595.
[14] S. Esplugas, J. Ggiménez, S. Contreras, E. Pascual, M. Rodriguez, Comparison of different advanced oxidation processes for phenol degradation, Water Res. 36 (2002) 1034–1042.
[15] M.A. Oturan, J.J. Aaron, Advanced oxidation processes in water/wastewater treatment: principles and applications. A review, Crit. Rev. Environ. Sci. Technol. 44 (2014) 2577–2641.
[16] J.J. Pignatello, E. Oliveros, A. MacKay, Advanced oxidation processes for organic contaminant destruction based on the Fenton reaction and related chemistry, Crit. Rev. Environ. Sci. Technol. 36 (2006) 1–84.
[17] O. Ganzenko, D. Huguenot, E.D. van Hullebusch, G. Esposito, M.A. Oturan, Electrochemical advanced oxidation and biological processes for wastewater

treatment: a review of the combined approaches, Environ. Sci. Pollut. Res. 21 (2014) 8493–8524.
[18] E. Brillas, C.A. Martinez-Huitle, Decontamination of wastewaters containing synthetic organic dyes by electrochemical methods. An updated review, Appl. Catal. B-Environ. 166 (2015) 603–643.
[19] E. Brillas, I. Sirés, M.A. Oturan, Electro-Fenton process and related electrochemical technologies based on Fenton's reaction chemistry, Chem. Rev. 109 (2009) 6570–6631.
[20] M.H. Zhou, Q.Q. Tan, Q. Wang, Y.L. Jiao, N. Oturan, M.A. Oturan, Degradation of organics in reverse osmosis concentrates by electro-Fenton process, J. Hazard. Mater. 215–216 (2012) 287–293.
[21] N. Oturan, J. Wu, H. Zhang, V.K. Sharma, M.A. Oturan, Electrocatalytic destruction of the antibiotic tetracycline in aqueous medium by electrochemical advanced oxidation processes: effect of electrode materials, Appl. Catal. B-Environ. 140 (2013) 92–97.
[22] I. Sirés, E. Brillas, M.A. Oturan, M.A. Rodrigo, M. Panizza, Electrochemical advanced oxidation processes: today and tomorrow. a review, Environ. Sci. Pollut. Res. 21 (2014) 8336–8367.
[23] M.A. Rodrigo, N. Oturan, M.A. Oturan, Electrochemically assisted remediation of pesticides in soils and water: a review, Chem. Rev. 114 (2014) 8720–8745.
[24] N. Oturan, E.D. van Hullebusch, H. Zhang, L. Mazeas, H. Budzinski, K. Le Menach, M.A. Oturan, Occurrence and of removal organic micropollutants in landfill leachates treated by electrochemical advanced oxidation processes, Environ. Sci. Technol. 44 (2014) 2577–2641.
[25] S. Shukla, M.A. Oturan, Dye removal via electrochemistry and oxidation using semiconductor oxides nanotubes, Environ. Chem. Lett. 13 (2015) 157–172.
[26] M.A. Oturan, An ecologically effective water treatment technique using electrochemically generated hydroxyl radicals for in situ destruction of organic pollutants. Application to herbicide 2,4-D, J. Appl. Electrochem. 30 (2000) 477–482.
[27] E. Mousset, L. Frunzo, G. Esposito, E.D. van Hullebusch, N. Oturan, M.A. Oturan, A complete phenol oxidation pathway obtained during electro-Fenton treatment and validated by a kinetic model study, Appl. Catal. B-Environ. 180 (2016) 189–198.
[28] N. Oturan, M. Zhou, M.A. Oturan, Metomyl degradation by electro-Fenton and electro-Fenton like processes: a kinetics study of the effect of the nature and concentration of some transition metal ions as catalyst, J. Phys. Chem. A 114 (2010) 10605–10611.
[29] A. El-Ghenymy, R.M. Rodríguez, E. Brillas, N. Oturan, M.A. Oturan, Electro-Fenton degradation of the antibiotic sulfanilamide with Pt/carbon-felt and BDD/carbon-felt cells. Kinetics reaction Intermediates and toxicity assessment, Environ. Sci. Pollut. Res. 21 (2014) 8368–8378.
[30] A. Özcan, Y. Şahin, A.S. Koparal, M.A. Oturan, A comparative study on the efficiency of electro-Fenton process in the removal of propham from water, Appl. Catal. B-Environ. 89 (2009) 620–626.
[31] H. Olvera-Vargas, N. Oturan, C.T. Aravindakumar, M.M. Sunil Paul, V.K. Sharma, M.A. Oturan, Electro-oxidation of the dye azure B: kinetics, mechanism and by-products, Environ. Sci. Pollut. Res. 21 (14) (2014) 8379–8838.
[32] S. Loaiza-Ambuludi, M. Panizza, N. Oturan, A. Özcan, M.A. Oturan, Electro-Fenton degradation of anti-inflammatory drug ibuprofen in hydroorganic medium, J. Electroanal. Chem. 702 (2013) 31–36.
[33] S. Ammar, M.A. Oturan, L. Labiadh, A. Guersalli, R. Abdelhedi, N. Oturan, E. Brillas, Degradation of tyrosol by a new electro-Fenton process using pyrite as heterogeneous ferrous iron as catalyst, Water Res. 74 (2015) 77–87.
[34] A.N. Subba Rao, V.T. Venkatarangaiah, Metal oxide-coated anodes in wastewater treatment, Environ. Sci. Pollut. Res. 21 (2014) 3197–3217.
[35] C.A. Martínez-Huitle, M.A. Rodrigo, I. Sires, O. Scialdone, Single and coupled electrochemical processes and reactors for the abatement of organic water pollutants: a critical review, Chem. Rev. 115 (2015) 13362–13407.
[36] F. Sopaj, M.A. Rodrigo, N. Oturan, F.I. Podvorica, J. Pinson, M.A. Oturan, Influence of the anode materials on the electrochemical oxidation efficiency. Application to oxidative degradation of the pharmaceutical amoxicillin, Chem. Eng. J. 262 (2015) 286–294.
[37] M. Panizza, G. Cerisola, Influence of anode material on the electrochemical oxidation of 2-naphthol. Part 2. Bulk electrolysis experiments, Electrochim. Acta 49 (2004) 3221–3226.
[38] B. Marselli, J. Garcia-Gomez, P.-A. Michaud, M.A. Rodrigo, Ch. Comninellis, Electrogeneration of hydroxyl radicals on boron-doped diamond electrodes, J. Electrochem. Soc. 150 (2003) D73–D79.
[39] C.A. Martinez-Huitle, S. Ferro, A. De Battisti, Electrochemical incineration of oxalic acid. Role of electrode material, Electrochim. Acta 49 (2004) 4027–4034.
[40] M. Panizza, G. Cerisola, Direct and mediated anodic oxidation of organic pollutants, Chem. Rev. 109 (2009) 6541–6569.
[41] D.M. de Araujo, C. Saez, C.A. Martinez-Huitle, P. Canizares, M.A. Rodrigo, Influence of mediated processes on the removal of Rhodamine with conductive-diamond electrochemical oxidation, Appl. Catal. B-Environ. 166 (2015) 454–459.
[42] V. Santos, J. Diego, M.J.A. Pacheco, A. Morao, A. Lopes, Electrochemical degradation of sulfonated amines on SI/BDD electrodes, Chemosphere 79 (2010) 637–645.
[43] N. Oturan, E. Brillas, M.A. Oturan, Unprecedented total mineralization of atrazine and cyanuric acid by anodic oxidation and electro-Fenton with a boron-doped diamond anode, Environ. Chem. Lett. 10 (2012) 165–170.
[44] M.O. Aust, F. Godlinski, G.R. Travis, X. Hao, T.A. McAllister, P. Leinweber, S. Thiele-Bruhn, Distribution of sulfamethazine, chlorotetracycline and tylosin in manure and soil of canadian feedlots after subtherapeutic use in cattle, Environ. Pollut. 156 (2008) 1243–1251.
[45] J.R. Reel, R.W. Tyl, A. Davis-Lawton, J.C. Lamb, Reproductive toxicity of sulfamethazine in Swiss CD-I mice during continuous breeding, Fundam. Appl. Toxicol. 18 (1992) 609–615.
[46] L.A. Poirier, D.R. Doerge, D.W. Gaylor, M.A. Miller, R.J. Lorentzen, D.A. Casciano, F.F. Kadlubar, B.A. Schwetz, An FDA review of sulfamethazine toxicity, Regul. Toxicol. Pharm. 30 (1999) 217–222.
[47] I. Sirés, J.A. Garrido, R.M. Rodríguez, E. Brillas, N. Oturan, M.A. Oturan, Catalytic behavior of the Fe3+/Fe2+ system in the electro-Fenton degradation of the antimicrobial chlorophene, Appl. Catal. B-Environ. 72 (2007) 382–394.
[48] A. Özcan, Y. Şahin, A.S. Koparal, M.A. Oturan, Carbon sponge as a new cathode material for the electro-Fenton process. Comparison with carbon felt cathode and application to degradation of synthetic dye Basic Blue 3 in aqueous medium, J. Electroanal. Chem. 616 (2008) 71–78.
[49] M. Turabik, N. Oturan, B. Gözmen, M.A. Oturan, Efficient removal of insecticide imidaclopride from water by electrochemical advanced oxidation processes, Environ. Sci. Pollut. Res. 21 (2014) 8387–8397.
[50] J. Beltran De Heredia, J. Torregrosa, J.R. Dominguez, J.A. Peres, Kinetic model for phenolic compound oxidation by Fenton's reagent, Chemosphere 45 (2001) 85–90.
[51] N. Oturan, S. Trajkovska, M.A. Oturan, M. Couderchet, J.J. Aaron, Study of the toxicity of diuron and its metabolites formed in aqueous medium during application of the electrochemical advanced oxidation process electro-Fenton, Chemosphere 73 (2008) 1550–1556.
[52] A. Dirany, S. Efremova Aaron, N. Oturan, I. Sirés, M.A. Oturan, J.J. Aaron, Study of the toxicity of sulfamethoxazole and its degradation products in water by a bioluminescence method during application of the electro-Fenton treatment, Anal. Bioanal. Chem. 400 (2011) 353–360.
[53] A. Dirany, I. Sirés, N. Oturan, A. Özcan, M.A. Oturan, Electrochemical treatment of Sulfachloropyridazine: kinetics, reaction pathways, and toxicity evolution, Environ. Sci. Technol. 46 (2012) 4074–4082.
[54] E.H. Calderon, J. Hahladakis, G. Foti, A. Katsaounis, Effectiveness factor for isopropanol oxidation on IrO2 based electrodes of different loading, Electrochim. Acta 55 (2010) 8215–8219.
[55] M. Diagne, N. Oturan, M.A. Oturan, Removal of methyl parathion from water by electrochemically generated Fenton's reagent, Chemosphere 66 (2007) 841–848.
[56] B. Balci, N. Oturan, R. Cherrier, M.A. Oturan, Degradation of atrazine in aqueous medium by electrocatalytically generated hydroxyl radicals. A kinetic and mechanistic study, Water Res. 43 (2009) 1924–1934.
[57] M. Li, C.P. Feng, Z.Y. Zhang, N. Sugiur, Efficient electrochemical reduction of nitrate to nitrogen using Ti/IrO_2-Pt anode and different cathodes, Electrochim. Acta 54 (2009) 4600–4606.
[58] B. Talhi, F. Monette, A. Azzouz, Effective and selective nitrate electroreduction into nitrogen through synergistic parameter interactions, Electrochim. Acta 58 (2011) 276–284.